Regular Article

PHYSICAL CHEMISTRY RESEARCH
Published by the
Iranian Chemical Society
www.physchemres.org
info@physchemres.org

Phys. Chem. Res., *Vol. 6, No. 3, 627-638, September 2018*
DOI: 10.22036/pcr.2018.121289.1475

Exploring the Interaction Mechanism of Coumarin with Bovine β-Casein: Spectrofluorometric and Molecular Modeling Studies

Z. Adibipour, N. Fani, A.-K. Bordbar* and M. Sahihi
Department of Chemistry, University of Isfahan, Isfahan 81746-73441, Iran
(Received 3 March 2018, Accepted 6 June 2018)

This paper is designed to examine the binding behavior of Coumarin with bovine β-casein (βCN) through fluorescence spectroscopy and molecular modeling techniques. The data analysis on fluorescence titration experiments at various temperatures represents the enthalpy driven nature for the formation of Coumarin-βCN complex and the prevailed role of hydrogen bonds and van der Waals interactions in the binding process. The results also represent the static quenching of tryptophan and dynamics quenching of tyrosine and phenylalanine residues due to the binding of Coumarin. It can be concluded from molecular docking studies that Coumarin binds to several polar and non-polar residues in the hydrophobic core of βCN with the binding energy of -6.96 kcal mol^{-1}. Finally, analysis of molecular dynamics (MD) simulation results suggested that the interactions between βCN and Coumarin are very stable and the binding of Coumarin restricted the flexibility of important residues in the binding site of this protein.

Keywords: β-casein (βCN), Coumarin, Molecular docking, Molecular dynamics simulation, Fluorescence spectroscopy

INTRODUCTION

Coumarin derivatives are found in cosmetic products, perfumes and food additives such as cinnamon and vanilla. These heterocyclic compounds are also found in many edible plants such as beans, lavender, licorice, strawberry, blackcurrant, apricot, sweet clover and cherry [1]. These derivatives as benzo-α-pyrone compounds have several characteristics such as high fluorescence quantum yield [2], large Stokes shift, excellent light stability and less toxicity [3]. The use of these compounds as fluorescent probes of pH, for detection of nitric oxide, nitroxide and hydrogen peroxide in food products is well established. The importance of these compounds also refers to their brilliant biological properties such as anticoagulant [4], free radical scavenger [5], antibacterial [6], antifungal [7], cytotoxic [8], anti-tumor, anti-viral, anti-inflammatory, antioxidant and antimicrobial activities [9].

The main problem with Coumarin, limiting its biological applications, is its tremendously low aqueous solubility and poor bioavailability. Several attempts have been made to encapsulate this compound in polymeric micelles and nanoparticles, liposomes, lipid-based nanoparticle and hydrogels in order to overcome its shortcomings [10].

Caseins are phosphoproteins that are produced from raw skimmed milk. The store and transport of bio-available metal ions such as calcium and phosphate through the formation of soluble assemblies are the main functions of caseins [11].

Beta-casein (βCN) as the predominant constituent of bovine milk casein has 209 residues in a single chain with the molecular weight of 23.983 kDa. Bovine βCN is a highly amphiphilic protein made up of a hydrophilic N-terminal part with a cluster of five phosphoryl residues and a hydrophobic C-terminal part [12]. The most common forms of this protein in dairy cattle breeds are A_1 and A_2, while B is the less common form [13-15]. It should be noted that bovine βCN is known as a dynamic protein with non-compact and flexible conformation [16].

*Corresponding author. E-mail: bordbar@chem.ui.ac.ir

The utilizing of βCN micelles as natural nano-delivery vehicles for lipid-soluble drugs have been reported in several studies. The easy digestion of βCN guarantees the easily release of encapsulated chemotherapeutics in the stomach [17]. Considering the ability of βCN for encapsulation of bioactive materials, it is of interest to gain further insight into the delivery mechanism of some drug candidates with bovine βCN nanoparticles. In this regard, some studies have investigated the binding properties of some compounds such as bisdemethoxycurcumin (BDMC) and Quercetin with βCN by using various experimental and computational techniques [18,19].

In the present work, a comprehensive study has been done on the interaction mechanism of Coumarin as a well-known bioactive compound with bovine βCN as a nano-carrier by spectrofluorimetric, molecular docking and molecular dynamics (MD) simulation techniques. The detail structural information regarding binding poses, binding affinities and the effect of Coumarin on the protein stability and secondary structure of βCN are reported here.

MATERIALS AND METHODS

Materials

Bovine βCN (>99%; Sigma-Aldrich, Germany) was dissolved in pH 7.0 phosphate buffer (PBS) containing 80 mM NaCl, 5.65 mM Na_2HPO_4 and 3.05 mM NaH_2PO_4 with an ionic strength of 0.1. All salts used for buffer preparation were of analytical grade and were dissolved in deionized water. To avoid large protein aggregation, the protein solution was filtered through a permeable membrane. The exact concentration of protein was determined spectrophotometrically using molecular absorption coefficient of 4.6 (1%) at 280 nm.

Coumarin with analytical grade was purchased from Merck Company and used without further purification. According to the low solubility of Coumarin in water, its stock solution was prepared in ethanol and the exact concentration was measured by determining its light absorption at λ_{max} ($\log\varepsilon_{274} = 4.2$).

Fluorescence Spectroscopy

Spectrofluorimeter RF-5000 (Shimadzu, Japan) was used for fluorescence measurements equipped with a xenon lamp source, a 1.0 cm quartz cell and a thermostat bath that kept temperature constant within ±0.1 °C. For spectrofluorometric experiments, 2 ml of βCN solution (11.5 μM) was put in quartz cell and titrated with specified volumes of Coumarin stock solution, over and over again. Emission spectra were separately recorded from 300 to 450 nm at an excitation wavelength of 295 nm and from 290 to 430 nm at an excitation wavelength of 280 nm. Both excitation and emission slit widths were set at 5 nm. It should be noted that emission spectrum of the βCN solution was measured as the control experiment and during the fluorescence measurements, ethanol concentration did not exceed over 1% v/v. The fluorescence titration experiments were run at four different temperatures ranging from 293K to 308 K and the gained results were analyzed for estimation of binding and thermodynamic quantities.

Preparation of βCN and Coumarin Structures

Since, the crystal structure of βCN does not exist in Protein Data Bank (PDB), in this paper, its structure was modeled using I-Threading ASSEmbly Refinement (TASSER) server which is a protein structure modeling approach based on the secondary structure enhanced profile-profile threading alignment (PPA) and the iterative implementation of the TASSER program [20]. Structural templates are first identified from the PDB by multiple threading approach LOMETS; full-length atomic models are then constructed by iterative template fragment assembly simulations. For query proteins that have no structurally related protein in the PDB library, the structure must be built from scratch by *ab initio* modeling [21]. This is a challenging task and success is limited to small proteins with < 120 amino acids [22]. Lastly, function in slights of the target is derived by threading the 3D models through protein function database BioLiP. I-TASSER server is in active development with the goal to provide the most accurate structural and functional predictions using state-of-the-art algorithms. The structure of βCN which was made with I-TASSER server contains 5 stands and 1 helix and other positions were made up of random coils.

To accomplish more stable and better structure of the model obtained from I-TASSER, a 50 ns molecular dynamic simulation was performed on the βCN structure using GROMACS 4.5.4 software package. The obtained

structure from the molecular dynamic simulation of βCN was used as the beginning point of molecular docking calculations.

The Coumarin structure was optimized using the quantum chemistry software Gaussian 03 and its calculation was approved at the 6-31G** level by employing the Becke three-parameters Lee-Yang-Parr (B3LYP) hybrid density functional theory.

Molecular Dynamics Simulation

MD simulation, as a very powerful method in modern molecular modeling, enables us to follow and understand structure and dynamics with extreme detail literally on scales where the motion of individual atoms can be tracked. This task will focus on the two most commonly used methods, namely energy minimization and molecular dynamics that respectively optimize the structure and simulate the natural motion of molecules. The Gromos43a1 was designated as force field [23] and 20680 SPC/E water molecules were employed according to the results of previous studies that revealed the SPC/E water model performs well in water box simulation [24]. The classical way to minimize edge effects in a finite system is to apply periodic boundary conditions. The atoms of the system supposed to be simulated were put into a space-filling cubic box of approximate dimensions 8.727 × 8.727 × 8.727 $Å^3$ surrounded by translated copies of itself. The adequate amount of sodium counter ions were exchanged with water molecules in order to neutralize the system for calculations. The added hydrogens and broken hydrogen bond network in water would lead to quite large forces and structure distortion if MD was started immediately. To eliminate these forces, a short energy minimization run is necessary. Hence, this run was done at first using the steepest descent method [25]. Two-step equilibration procedures are needed to relax the solvent and ions while keeping the protein atom positions restrained. This was accomplished in two phases: 100 ps NVT followed by 100 ps NPT ensembles. The dynamics were performed at conditions of 300 K and 1.0 bar which is close to the circumstances of most laboratory environments. A standard cut-off of 1.0 nm for both of the neighbor list generation and the Coulomb and Lennard-Jones interactions were selected. Energies and other statistical data were stored every 10 steps and the more expensive Particle-Mesh-Ewald summation was chosen for electrostatic interactions [26].

Molecular Docking Calculation

The molecular docking calculations were carried out to visualize the binding site of Coumarin in βCN and to determine the involved residues in the interaction. Docking calculations were accomplished using AutoDock 4.2.2 package which is an automated procedure for predicting the interactions of ligands with biomacromolecular targets [27]. Protein model was first modified by adding all hydrogens using the builder module of Autodock. The macromolecule was kept rigid, while all the torsional bonds of ligand were set free to rotate. First, a blind docking with 126 lattice points along X, Y and Z axes was performed to find the binding site of ligand to βCN. After determination the binding site, the dimensions of the grid map were selected 60 points with a grid point spacing of 0.375 Å to allow the ligand to rotate freely. By using the Lamarckian genetic algorithm (LGA) method, 200 separated docking calculations consisted of the maximum 25,000,000 energy evaluations were performed. The clustering of docking results from each of the 200 calculations was done on the basis of root mean square deviations (*RMSD*) between the Cartesian coordinates of the ligand atoms also were ranked according to the free energy of binding. The structure with the lowest free energy of binding in the highest populated cluster was chosen as the optimal docking pose.

RESULTS AND DISCUSSION

Fluorescence Spectroscopy

In order to identify the binding mechanism, the measurement of intrinsic fluorescence of βCN in the presence of various amounts of Coumarin was performed. Trp residue of βCN which can provide important information about the formation of Coumarin-βCN complex was mainly placed in the hydrophobic region of this protein. Figure 1a shows fluorescence emission spectra of βCN in various concentrations of Coumarin at 293 K. The quenching effect of Coumarin on fluorescence spectrum of βCN is observed in this figure. Fluorescence quenching refers to any process which decreases the fluorescence intensity of a given substance. The processes such as

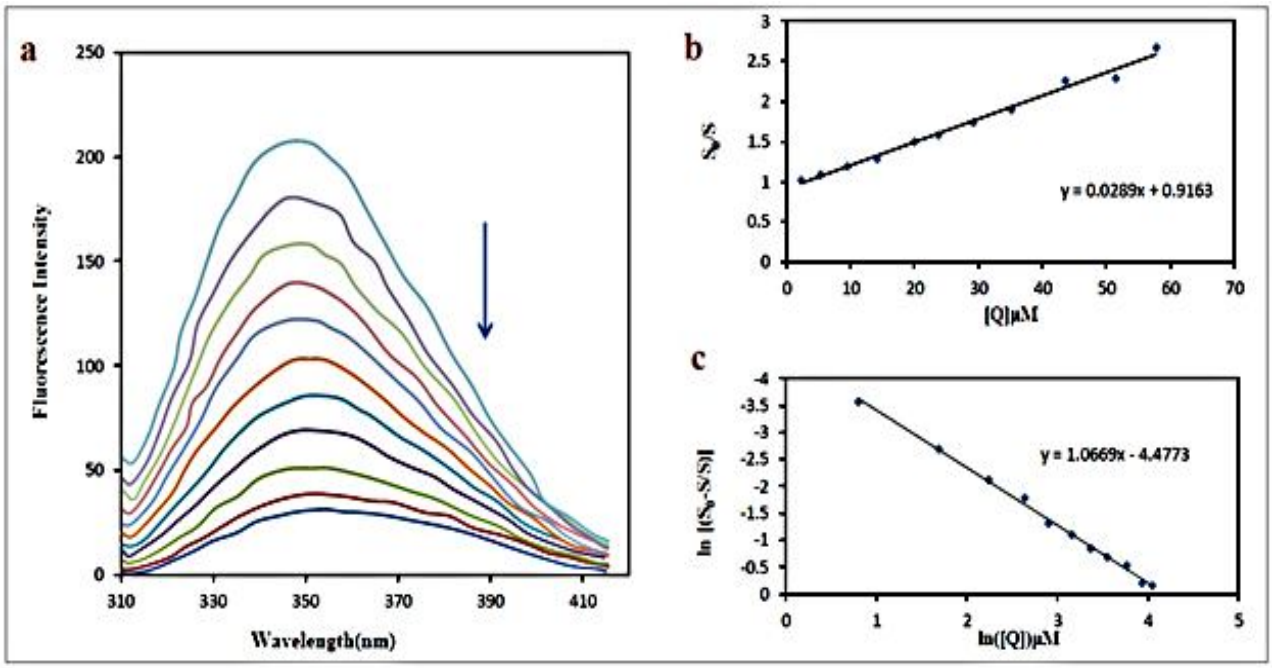

Fig. 1. (a) Fluorescence quenching of βCN solution by Coumarin in PBS pH 7, T = 293K, λ_{ex} = 295 nm and [βCN] = 11.5 μM. The concentration of Coumarin was increased in the direction of arrow. (b) The variation of S_0/S *vs.* total concentration of Coumarin. (c) The variation of ln[(S_0 - S/S)] *vs.* ln[Q].

Table 1. Binding Constants, Stern-Volmer Constants, and the Number of Binding Sites for Interaction of Coumarin with βCN in PBS pH 7

T (K)	$K_a \times 10^4$ (M^{-1})	$K_{sv} \times 10^4$ (M^{-1})	R^2	*n*
293	1.14 ± 0.16	2.89 ± 0.10	0.99	1.07 ± 0.02
298	1.05 ± 0.15	2.88 ± 0.11	0.99	1.07 ± 0.04
303	0.96 ± 0.25	2.72 ± 0.08	0.98	1.04 ± 0.02
308	0.89 ± 0.11	2.70 ± 0.06	0.99	1.00 ± 0.02

excited state reactions, energy transfer, complex-formation and collisional quenching can result in quenching. There are two main mechanisms for fluorescence quenching usually called as dynamic and static. Collisional (dynamic) quenching occurs when the excited fluorophore experiences contact with an atom or molecule that can facilitate non-radiative transitions to the ground state. In some cases, the fluorophore can form a stable complex with another molecule. The fluorophore is statically quenched, if this ground-state complex is non-fluorescent. In the simplest case of dynamic and static quenching, the following relation, called the Stern-Volmer equation, holds (Juan

et al., 2044):

$$S_0/S = 1 + K_{sv}[Q] \quad (1)$$

where S_0 and S are the total area under the emission spectrum in the absence and presence of quencher, [Q] is the quencher concentration and K_{SV} is the Stern-Volmer quenching constant. Plot of S_0/S *versus* [Coumarin] at 293 K is shown in Fig. 1b. The high linearity of this plot represents a good agreement between the results and the Stern-Volmer equation within the investigated concentrations.

The calculated K_{sv} at four temperatures ranging from 293-308 K is represented in Table 1. The decreasing of K_{sv} values with temperature designates static quenching mechanism [28].

In order to calculate the number of binding sites of the ligand on the surface of the protein (n) and the associative binding constant (K_a), the following equation can be used [28]:

$$\ln[(S_0 - S)/S] = \ln K_a + n\ln[Q] \quad (2)$$

Figure 1c shows the corresponding plots of above equation to estimate the values of K_a and n for binding of Coumarin to βCN. The calculated values of K_a and n at four temperatures are presented in Table 1. The estimated K_a values were used for calculation of the thermodynamic parameters of reaction at various temperatures.

The values of binding constants indicate the high affinity for binding of Coumarin to βCN. The energetics of protein-ligand equilibrium can be conveniently characterized by three thermodynamic parameters; the standard Gibbs free energy, $\Delta G°$, the standard molar enthalpy, ΔH^0, and the standard molar entropy, $\Delta S°$. $\Delta G°$ can be calculated from the equilibrium constant, K_a, of the reaction using the relationship, $\Delta G° = -RT \ln K_a$, where R and T are gas constants and the absolute temperature, respectively. Therefore, the temperature dependent thermodynamic parameters were calculated to elucidate the interaction mechanism. The standard enthalpy and entropy changes of binding could be estimated from the following equations, based on the binding constants at different temperatures:

$$\Delta H° = d(\Delta G°/T)/d(1/T) \quad (3)$$

$$\Delta S° = (\Delta H° - \Delta G°)/T \quad (4)$$

The plot of $\Delta G°/T$ *vs*. $1/T$ is shown in Fig. S1 and their calculated thermodynamic parameters at different temperatures ranging from 293-308 K are reported in Table 2.

Hydrophobic, electrostatic, van der Waals interactions and hydrogen bonds are the main driving forces in the binding phenomena that could be designated from the thermodynamic parameters. The sign and magnitude of thermodynamic parameters corresponding to these driving forces in the protein association process were characterized by Ross and Subramanian [29].

It can be concluded from Table 2 that the binding procedure between Coumarin and βCN is spontaneous and mainly enthalpy driven. In advance, the negative values obtained for $\Delta H°$ and $\Delta S°$ indicates the significance of hydrogen bonding and van der Waals interactions in the binding process. Therefore, it can be concluded that both hydrogen bonding and van der Waals interactions play an essential role in the binding of Coumarin to βCN.

Finally, to identify the quenching mechanism of tyrosine and phenylalanine residues of βCN, the intrinsic fluorescence of protein was measured in the presence of various amounts of Coumarin at four temperatures ranging from 293-308 K at the excitation wavelength of 280 nm. With respect to Fig. S1, a positive deviation from linearity of S_0/S *vs*. [Coumarin] plot is observed. In fact, this usually happens when two different mechanisms of quenching (*i.e.* dynamic and static quenching) occur synchronously. Hence, the static quenching mechanism for tryptophan and dynamics for tyrosine and phenylalanine could be concluded.

Fluorescence Resonance Energy Transfer (FRET) from βCN to Coumarin

Fluorescence resonance energy transfer (FRET) is a mechanism describing energy transfer between two light-sensitive molecules (chromophores). A donor chromophore, initially in its electronic excited state, may transfer energy to an acceptor chromophore through the nonradiative dipole-dipole coupling. The efficiency of this phenomenon

Table 2. Thermodynamic Parameters for the Association of Coumarin with βCN

T (K)	$\Delta G°$ (kJ mol^{-1})	$\Delta G°$ (kJ mol^{-1})	R^2	$\Delta S°$ (J mol^{-1} K^{-1})
293	-23.91 ± 0.33	-56.71 ± 2.18	0.99	-193.28 ± 2.50
298	-23.33 ± 0.33	-56.71 ± 2.18	0.99	-190.05 ± 2.51
303	-22.73 ± 0.60	-56.71 ± 2.18	0.99	-186.92 ± 2.78
308	-22.15 ± 0.28	-56.71 ± 2.18	0.99	-183.89 ± 2.45

is inversely proportional to the sixth power of the distance between donor and acceptor, making FRET extremely sensitive to small changes in distance. Measurements of FRET efficiency could be determined if two fluorophores are within a certain distance of each other.

Fluorescence quenching of βCN by Coumarin indicated the possibility of energy transfer between the protein and the bound Coumarin. In the present study, we prepared a solution containing the equimolar concentration of βCN and Coumarin (5 μM), and its UV-Vis absorption and fluorescence spectra were recorded. There is a good overlap between the emission spectrum of βCN and the absorption spectrum of Coumarin (Fig. s1). The efficiency of energy transfer can be calculated by using Eq. (5), where F_0 and F are the fluorescence intensity of β-casein in the absence and presence of Coumarin, respectively, r is the distance from the bound ligand to the tryptophan residue and R_0 is the Forster critical distance at which 50% of the excitation energy is transferred to the acceptor and can be obtained from Eq. (6) using $K^2 = 2/3$, N = 1.53, and φ = 1.49 [28], where K^2 is a factor describing the relative orientation of the transition dipoles of the protein donor and ligand acceptor, N is the average refractive index of the medium in the wavelength range where the spectral overlap is significant, and φ is the fluorescence quantum yield of the protein donor. Overlap integral (J) expresses the extent of overlap between the normalized fluorescence emission spectrum of the protein donor and the ligand acceptor absorption spectrum and is given by Eq. (7). In this equation, $F(\lambda)$ is the fluorescence intensity of the donor at wavelength λ and is dimensionless and $\varepsilon(\lambda)$ is the molar absorption coefficient of the acceptor at wavelength λ. In this study, the calculated value for J was 7.389×10^{-15} (cm^3 M^{-1}). By using the obtained value for E from Eq. (5) (0.204) and R_0 from Eq. (6) (63.250 nm), the r value was calculated to equal to 4.078 nm. It can be seen that the distance from the bound ligand to the tryptophan residue is less than 7 nm indicating a non-radiative energy transfer mechanism for quenching [30]. Moreover, the value of r is higher than the respective critical distance (R_0), hence, the static quenching is more likely responsible than the dynamic mechanism that is in agreement with our conclusion corresponding to the reducing of K_{sv} with temperature. Moreover, the short distance value between bound ligand and the tryptophan residue represents the significant interaction between Coumarin and βCN.

$$E = 1 - \frac{F}{F_0} = \frac{R_0^6}{R_0^6 + r^6} \tag{5}$$

$$R_0^6 = 8.79 \times 10^{-25} K^2 N^{-4} \varphi J \tag{6}$$

$$J = \frac{\sum F(\lambda)\varepsilon(\lambda)\lambda^4 \Delta\lambda}{\sum F(\lambda)\Delta\lambda} \tag{7}$$

Molecular Docking Study

Molecular docking studies were implemented to understand the binding site location and the best conformation of Coumarin for binding to βCN using binding free energy assessment. Estimated energies by AutoDock are described by intermolecular energy, internal energy, and torsional free energy. Docking studies showed

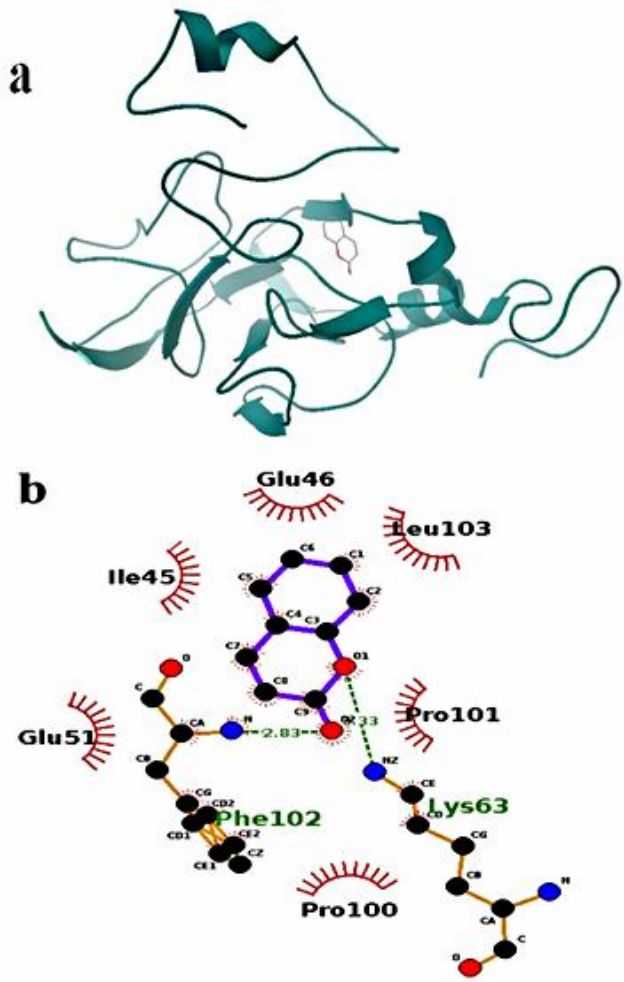

Fig. 2. (a) Ribbon model of Coumarin-βCN complex. (b) Detailed view of the interactions of Coumarin with βCN.

that Coumarin binds to the hydrophobic core of βCN. The representative build derived from the best pose of Coumarin with the minimal binding energy of -6.96 kcal mol^{-1} is shown in Fig. 2a.

As this figure shows, βCN has 3 helixes and 8 strands in its structure which were held together with random coils. Coumarin is nearby to some hydrophobic residues in the core of βCN such as Leu103, Pro101, Pro100, Phe102 and Ile45. Moreover, some polar residues such as Glu51, Glu46, and Lys63 are in the neighborhood of Coumarin. The docking results showed that Coumarin is able to form a hydrogen bond interaction with Phe102 residue, and therefore, this residue plays a significant role in stabilizing the complex (Fig. 2b).

Molecular Dynamics Simulation Study

The lowest energy structure of Coumarin resulting from docking calculation was selected for the initial structure of 50 ns MD simulation on the ligand-protein complex. To this end, force field parameters of ligand were obtained from PRODRG web server [31].

In order to investigate the stability of the βCN-Coumarin complex and determination of the types of interactions involved in the binding reaction, some system properties including root mean square deviations (*RMSD*), radius of gyration (R_g), secondary structure, root mean square fluctuations (*RMSF*), accessible surface area of protein and hydrogen bonds were investigated.

Root mean square deviations. The standard way to

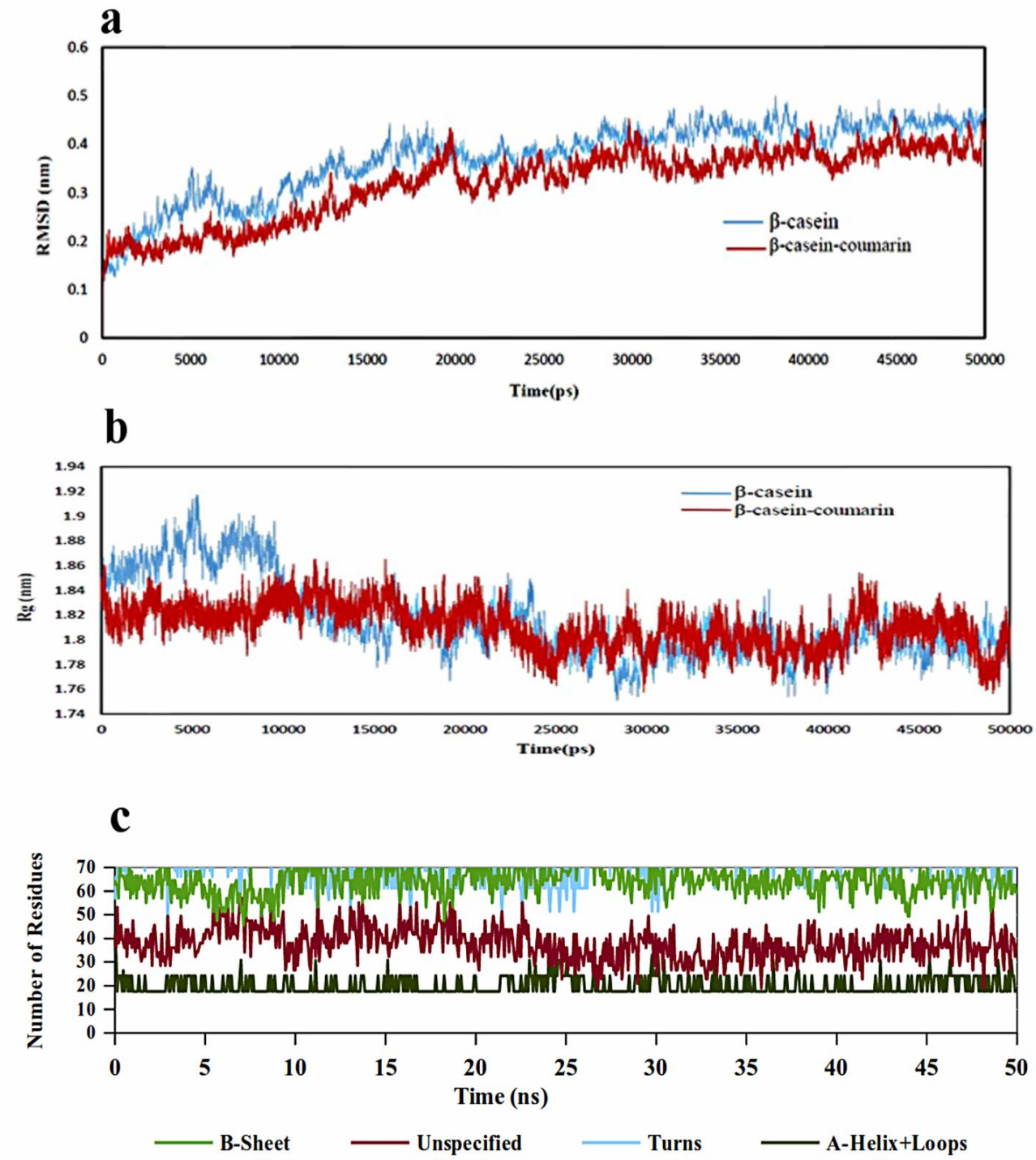

Fig. 3. (a) Root mean square deviation (nm) of backbone atoms of βCN in the absence and presence of Coumarin. (b) Time dependence of the radius of gyration (Rg) for the backbone atoms of βCN during the simulation in the absence and presence of Coumarin. (c) The variation of the secondary structure *vs*. time for the βCN-Coumarin complex system.

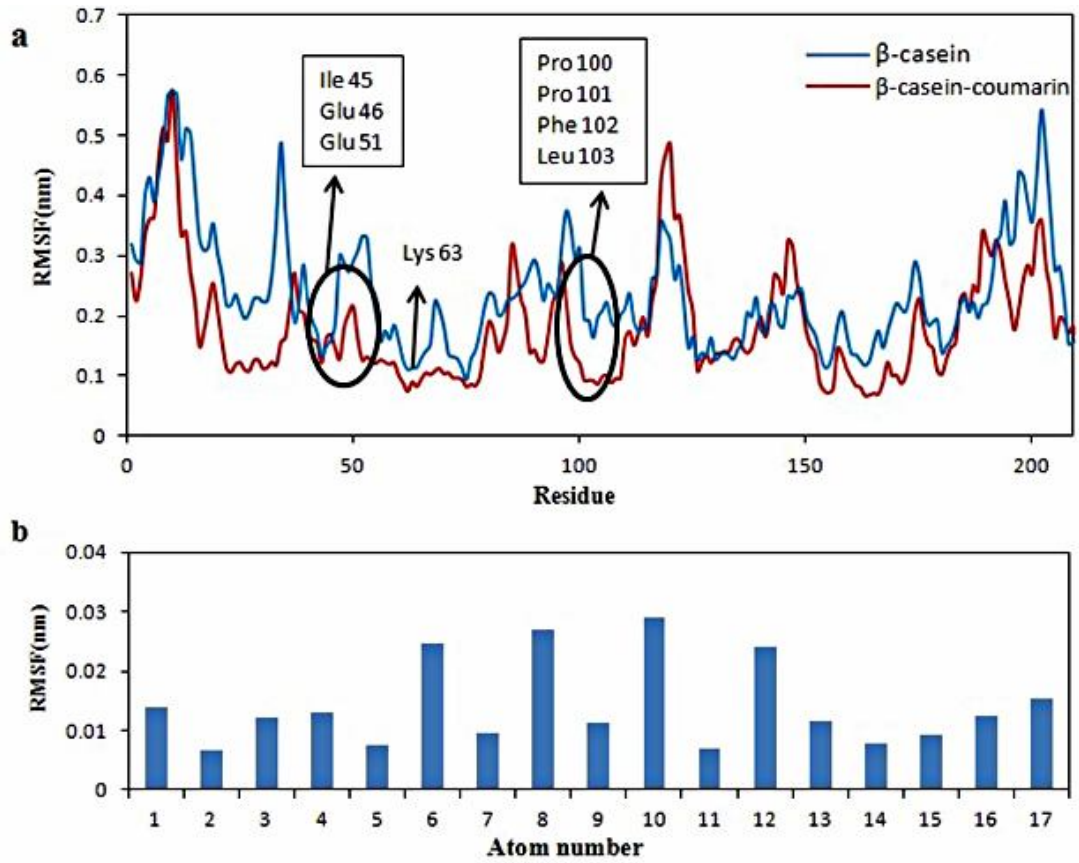

Fig. 4. (a) RMSF of the protein residues from their time-averaged positions for free (blue) and bound (red) βCN. (b) RMSF of Coumarin atoms during the simulation.

measure the trajectory stability for both βCN and βCN-Coumarin complex is to calculate the root-mean-square deviations (*RMSD*) of backbone atoms of protein from the initial structure, as a function of time. It can be seen in Fig. 3a that the *RMSD* of protein increases pretty rapidly in the first part of the simulation, but it reaches to equilibrium and oscillates around the average value after about 20000 ps simulation time. In another word, for most of the times (between 20 and 50 ns) the *RMSD* profile of protein backbone atoms shows similar trends for both systems indicating their stability and equilibration. The mean *RMSD* values of protein backbone atoms from last 20 ns trajectory were 0.435 ± 0.030 and 0.523 ± 0.021 nm for βCN and βCN-Coumarin complex, respectively.

Radius of gyration. The radius of gyration (R_g) is a factor which designates the compactness of the system. The radius of gyration of the free and bound form of the protein was determined and plotted as a function of time. As shown in Fig. 3b, in both systems, the R_g values are stabilized at about 25000 ps, indicating the achievement of equilibrium after this time. As seen in this figure, for both systems, the radius of gyration of backbone atoms does not change significantly. This implies a small decrease in the compacting of the βCN structure during the simulation.

Secondary structure analysis. The secondary structure of βCN was calculated for each frame with DSSP program [32]. The result provides the α-helix content and other secondary structures of the protein. It is easy to notice that the main secondary structure of the protein in the presence of Coumarin maintains rather stable during whole MD simulation time (Fig. 3c).

The surface area of protein. Gases command

computes hydrophobic, hydrophilic and total solvent accessible surface area. The program will ask for a group for the surface calculation and a group for the output. The calculation group should always consist of all non-solvent atoms in the system. The output group can be the whole or part of the calculation group. The area of the protein in the presence and absence of Coumarin indicates that the surface of βCN due to interaction with Coumarin does not change significantly and this is in agreement with our conclusion corresponding to the radius of gyration (Fig. S2).

Hydrogen bonds. G-h bond command computes the number of hydrogen bonds. The maximum of three hydrogen bonds can be formed between Coumarin and βCN, however, most of the time, only one hydrogen bond is formed which is in good agreement with the docking results (Fig. S2).

Root mean square fluctuations. Vibrations around the equilibrium are not random, and depend on local structure flexibility. The time-averaged root mean square fluctuation (*RMSF*) values of free βCN and βCN-Coumarin complex were calculated, and the results were plotted against residue numbers (Fig. 4a). As seen in this figure, the binding of Coumarin restricted the conformational space explored by βCN as assessed by a general reduction of the protein *RMSF*. In the other word, the overall reduction in the *RMSF* values reveals that binding of Coumarin reduces βCN flexibility. The particular regions directly in contact with Coumarin, including Leu103, Pro101, Glu51, Pro100, Phe102, Glu46, Phe48, Lys47, Ile45, Lys63 and Pro168 residues (pointed in Fig. 4a) show the more significant reduction in RMSF that is related to intermolecular interactions of these residues with the ligand.

Moreover, the RMSF of the atomic positions of the Coumarin was calculated to examine its conformational variation (Fig. 4b). The results indicated that the Coumarin atoms show limited fluctuations (<0.03 nm). Hence, it can be concluded that the interactions of βCN and Coumarin were stable during the simulation time.

CONCLUSIONS

This paper describes the interaction mechanism of Coumarin with bovine β-Casein using fluorescence spectroscopy, molecular docking, and MD simulation studies. The fluorescence studies presented here revealed the static quenching of βCN fluorescence and the formation of 1:1 complex between this protein and Coumarin. The negative values of both enthalpy and entropy changes by running the experiments at various temperatures recommend that hydrogen bonding and van der Waals interactions play important roles in the binding process. Moreover, fluorescence quenching studies revealed the existence of single binding site for Coumarin on βCN with relatively high binding affinity. Förster energy transfer measurements suggested that the distance between bound Coumarin and Trp143 residue is higher than the respective critical distance. Therefore, the static quenching is more likely responsible for fluorescence quenching of βCN. The results of computational docking studies indicated that Coumarin probably binds to the hydrophobic core of βCN and the interaction proceeds through van der Waals and hydrogen bond interactions. The RMSD and radius of gyration profiles obtained by MD calculations demonstrated the stability of βCN-Coumarin complex during the simulation time. Analysis of MD data represented the insignificant change of secondary and tertiary structures of βCN due to the binding of Coumarin. Finally, the RMSF profiles and hydrogen bond analysis revealed the insignificant movement of Coumarin from its pose during the whole MD simulation time. To sum up, all experimental and molecular modeling results reciprocally supported each other and clarified that βCN seems to be the promising Coumarin carrier.

ACKNOWLEDGMENTS

The financial support of the Research Council of University of Isfahan and Iran National Science Foundation (grant number 93013717) are gratefully acknowledgment.

Conflict of interest statement

We have no conflicts of interest.

List of Abbreviations

βCN: β-Casein
RMSD: Root Mean Square Deviations
RMSF: Root Mean Square Fluctuations
BDMC: BisDeMethoxy Curcumin

MD: Molecular Dynamics
TASSER: Threading Assembly Refinement

REFERENCES

[1] Marles, R. J.; Compadre, C. M.; Farnsworth, N. R., Coumarin in vanilla extracts: Its detection and significance. *Econ. Bot.* **1987**, 41-47, DOI: 10.1007/BF02859345.

[2] Zahradník, M., The Production and Application of Fluorescent Brightening Agents. Wiley, 1982

[3] Bullock, S. J.; Felton, C. E.; Fennessy, R. V. *et al.*, Coumarin-based luminescent ligand that forms helicates with dicationic metal ions. *Dalt. Trans.* **2009**, 10570, DOI: 10.1039/b913103e.

[4] Ghazaryan, A. V.; Khatchadourian, A. S.; Karagyozyan, M. K. *et al.,* Peculiarities of the anticoagulant properties for the newly synthesized preparations of coumarin-related compounds. *Cardiovasc Hematol Disord. Drug Targets* **2007**, *7*, 170-3.

[5] Kancheva, V. D.; Boranova, P. V.; Nechev, J. T.; Manolov, I. I., Structure-activity relationships of new 4-hydroxy bis-coumarins as radical scavengers and chain-breaking antioxidants. *Biochimie* **2010**, *92*, 1138-1146, DOI: 10.1016/j.biochi.2010.02.033.

[6] Morabito, G.; Trombetta, D.; Singh Brajendra, K. *et al.*, Antioxidant properties of 4-methylcoumarins in *in vitro* cell-free systems. *Biochimie* **2010**, *92*, 1101-1107, DOI: 10.1016/j.biochi.2010.04.017.

[7] Grimm, E. L.; Brideau, C.; Chauret, N. *et al.*, Substituted coumarins as potent 5-lipoxygenase inhibitors. *Bioorganic Med. Chem. Lett.* **2006**, *16*, 2528-2531, DOI: 10.1016/j.bmcl.2006.01.085.

[8] Resch, M.; Steigel, A.; Chen, Z.; Bauer, R., 5-Lipoxygenase and cyclooxygenase-1 inhibitory active compounds from atractylodes lancea. *J. Nat. Prod.* **1998**, *61*, 347-350, DOI: 10.1021/np970430b.

[9] Bansal, Y.; Ratra, S.; Bansal, G. *et al.*, Design and synthesis of coumarin substituted oxathiadiazolone derivatives having anti-inflammatory activity possibly through p38 MAP kinase inhibition. *J. Iran. Chem. Soc.* **2009**, DOI: 10.1007/BF03246527.

[10] Rassu, G.; Nieddu, M.; Bosi, P. *et al.*, Encapsulation and modified-release of thymol from oral microparticles as adjuvant or substitute to current medications. *Phytomedicine* **2014**, *21*, 1627-1632, DOI: 10.1016/j.phymed.2014.07.017.

[11] Bhattacharyya, J.; Das, K. P., Molecular chaperone-like properties of an unfolded protein, alpha(s)-casein. *J. Biol. Chem.* **1999**, *274*, 15505-9.

[12] De Kruif, C. G.; Grinberg, V. Y., Micellisation of casein. *Colloids Surfaces A Physicochem. Eng. Asp.* **2002**, *210*, 183-190, DOI: 10.1016/S0927-7757(02)00371-0.

[13] Eigel, W. N.; Butler, J. E.; Ernstrom, C. A. *et al.*, Nomenclature of proteins of cow's milk: Fifth Revision. *J. Dairy Sci.* **1984**, *67*, 1599-1631, DOI: 10.3168/jds.S0022-0302(84)81485-X.

[14] Kamiński, S.; Cieślińska, A.; Kostyra, E., Polymorphism of bovine beta-casein and its potential effect on human health. *J. Appl. Genet* **2007**, *48*, 189-198, DOI: 10.1007/BF03195213.

[15] Keating, A. F.; Smith, T. J.; Ross, R. P.; Cairns, M. T., A note on the evaluation of a beta-casein variant in bovine breeds by allele-specific PCR and relevance to β-casomorphin. *Irish J. Agric. Food Res.* **2008**, *47*, 99-104.

[16] O'Connell, J. E.; Grinberg, V. Y.; De Kruif, C. G., Association behavior of??-casein. *J. Colloid Interface Sci.* **2003**, *258*, 33-39, DOI: 10.1016/S0021-9797(02)00066-8

[17] Semo, E.; Kesselman, E.; Danino, D.; Liveny, Y., Casein micelle as a natural nano-capsular vehicle for nutraceuticals. *Food Hydrocoll* **2007**, *21*, 936-942, DOI: 10.1016/j.foodhyd.2006.09.006.

[18] Mehranfar, F.; Bordbar, A. K.; Fani, N.; Keyhanfar, M., Binding analysis for interaction of diacetylcurcumin with β-casein nanoparticles by using fluorescence spectroscopy and molecular docking calculations. *Spectrochim. Acta Part A Mol. Biomol. Spectrosc.* **2013**, *115*, 629-635, DOI: 10.1016/j.saa.2013.06.062.

[19] Mehranfar, F.; Bordbar, A. K.; Parastar, H., A combined spectroscopic, molecular docking and molecular dynamic simulation study on the interaction of quercetin with β-casein nanoparticles. *J. Photochem. Photobiol. B Biol.* **2013**, *127*, 100-

107. DOI: ttp://dx.doi.org/10.1016/j.jphotobiol. 2013.07.019.

[20] Sokkar, P.; Mohandass, S.; Ramachandran, M., Multiple templates-based homology modeling enhances structure quality of AT1 receptor: Validation by molecular dynamics and antagonist docking. *J. Mol. Model* **2011**, *17*, 1565-1577, DOI: 10.1007/s00894-010-0860-z.

[21] Liwo, A.; Lee, J.; Ripoll, D. R. *et al.*, Protein structure prediction by global optimization of a potential energy function. *Proc. Natl. Acad. Sci. USA* **1999**, *96*, 5482-5485, DOI: 10.1073/ pnas.96.10.5482.

[22] Jain, H. D.; Zhang, C.; Zhou, S. *et al.*, Synthesis and structure-activity relationship studies on tryprostatin A, an inhibitor of breast cancer resistance protein. *Bioorg. Med. Chem.* **2008**, *16*, 4626-4651, DOI: 10.1016/j.bmc.2008.02.050.

[23] van der Spoel, D.; Lindahl, E.; Hess, B. *et al.*, Gromacs User Manual version 4.0. Manuals 308 2008, DOI: 10.1007/SpringerReference_28001.

[24] Rivail, L.; Chipot, C.; Maigret, B. *et al.*, Large-scale molecular dynamics of a G protein-coupled receptor, the human 5-HT4 serotonin receptor, in a lipid bilayer. *J. Mol. Struct. Theochem.* **2007**, *817*, 19-26, DOI: 10.1016/j.theochem.2007.04.012.

[25] Berendsen, H. J. C.; Grigera, J. R.; Straatsma, T. P., The missing term in effective pair potentials. *J. Phys. Chem.* **1987**, *91*, 6269-6271, DOI: 10.1021/ j100308a038.

[26] York, D. M.; Darden, T. A.; Pedersen, L. G., The effect of long? range electrostatic interactions in simulations of macromolecular crystals: A comparison of the Ewald and truncated list methods. *J. Chem. Phys.* **1993**, *99*, 8345-8348, DOI: 10.1063/ 1.465608.

[27] Morris, G. M.; Goodsell, D. S.; Halliday, R. S. *et al.*, Automated docking using a Lamarckian genetic algorithm and an empirical binding free energy function. *J. Comput. Chem.* **1998**, *19*, 1639-1662, DOI: 10.1002/(SICI)1096-987X(19981115)19:14< 1639::AID-JCC10>3.0.CO;2-B.

[28] Lakowicz, J. R., Principles of Fluorescence Spectroscopy 2006.

[29] Eftink, M. R.; Ghiron, C. A., Fluorescence quenching studies with proteins. *Anal. Biochem.* **1981**, *114*, 199-227.

[30] Vörös, J., The density and refractive index of adsorbing protein layers. *Biophys.* **2004**, *87*, 553-561, DOI: 10.1529/biophysj.103.030072.

[31] van Aalten, D. M.; Bywater, R.; Findlay, J. B. *et al.*, PRODRG, a program for generating molecular topologies and unique molecular descriptors from coordinates of small molecules. *J. Comput. Aided Mol. Des.* **1996**, *10*, 255-62, DOI: 10.1007/ BF00355047.

[32] Kabsch, W.; Sander, C., Dictionary of protein secondary structure: Pattern recognition of hydrogen bonded and geometrical features. *Biopolymers* **1983**, *22*, 2577-2637, DOI: 10.1002/bip.360221211.